Electronic Supplementary Information to

Spin Labels for ^{19}F ENDOR Distance Determination: Resolution, Sensitivity and Distance Predictability

Alexey Bogdanov[1], Longfei Gao[2], Arina Dalaloyan[1], Wenkai Zhu[3], Manas Seal[1], Xun-Cheng Su[4], Veronica Frydman[5], Yangping Liu[2], Angela M. Gronenborn[3], Daniella Goldfarb[1*]*

*daniella.goldfarb@weizmann.ac.il *alexey.bogdanov@weizmann.ac.il

[1] Department of Chemical and Biological Physics, The Weizmann Institute of Science, P. O. Box 26, Rehovot, 7610001, Israel

[2] Tianjin Key Laboratory on Technologies Enabling Development of Clinical Therapeutics and Diagnostics, School of Pharmacy, Tianjin Medical University, Tianjin, 300070 P. R. China

[3] Department of Structural Biology, University of Pittsburgh, 4200 Fifth Ave, Pittsburgh, PA 15260, United States

[4] State Key Laboratory of Elemento-Organic Chemistry, Nankai University, Tianjin 300071 P. R. China

[5] Department of Chemical Research Support, The Weizmann Institute of Science, P. O. Box 26, Rehovot, 7610001, Israel

Table of contents

S1. Characterization of trityl spin labels

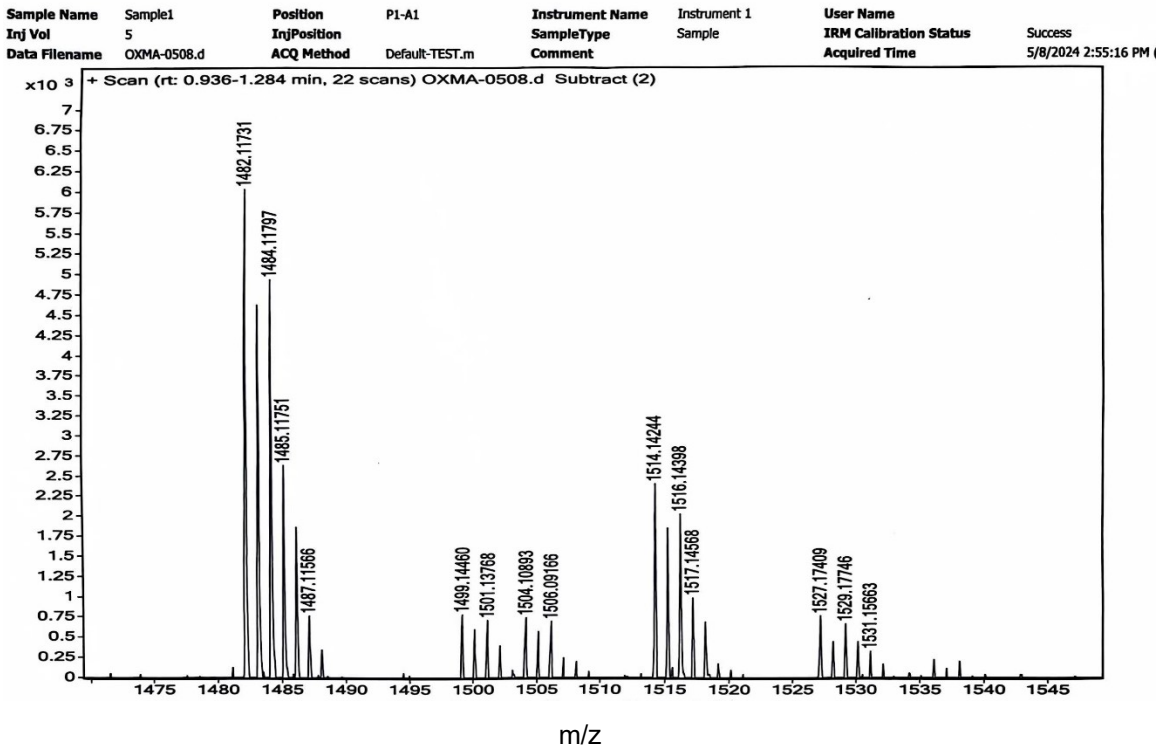

Fig. S1. HRMS(ESI+) m/z: [M]+ . Calculated for $C_{58}H_{69}N_2O_{19}S_{12}^+$:1482.1177; found: 1482.1173.

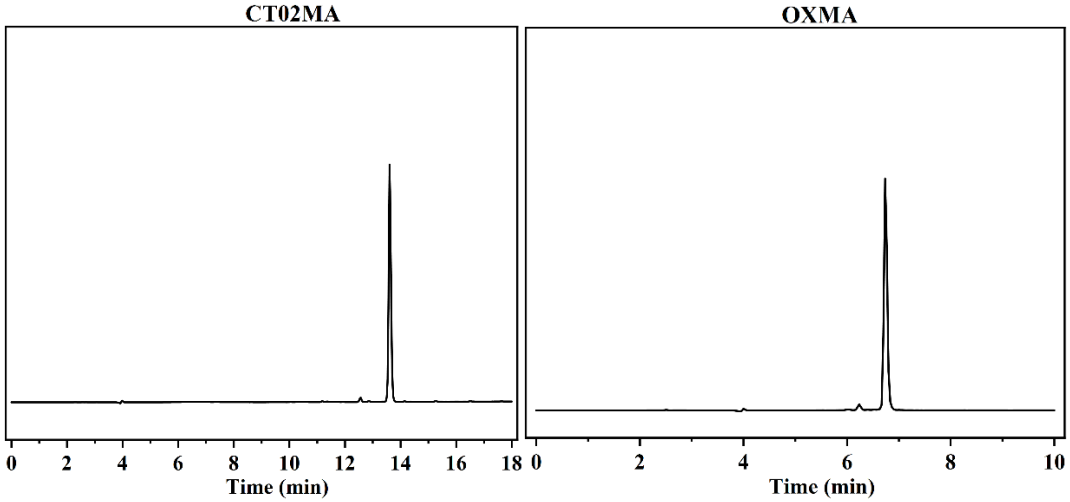

Fig. S2. HPLC chromatograms of CT02MA and OXMA. HPLC (ODS-3, 20 mM ammonium acetate/acetonitrile = 90:10-10:90, flow rate = 1.0 mL/min, λ = 254 nm), t_R = 13.7 min (CT02MA), 6.7 min (OXMA). The purities of these radicals were determined to be above 95%.

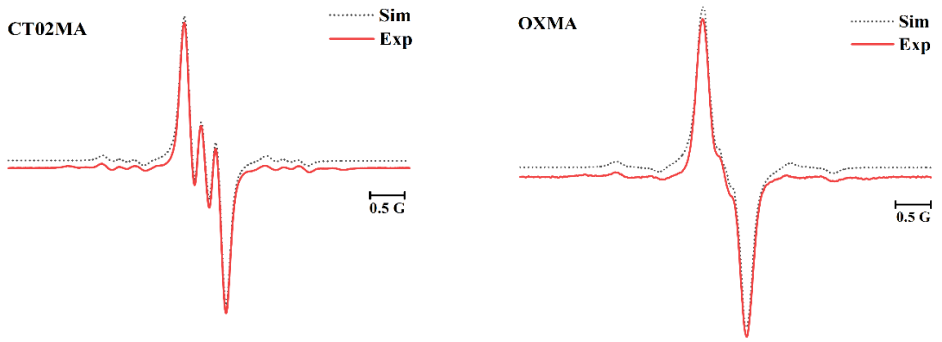

Fig. S3. Experimental (red solid line) and simulated (black dotted line) EPR spectra of CT02MA and OXMA in PBS at room temperature under anaerobic conditions.

HPLC analysis was performed using a CoulArray chromatography system from Shimadzu Analytical LC-20AT(JAPAN) with a C18 GL Science Inertsil ODS-3 column (250*4.6 mm, 5 µm). Elution was achieved using a gradient of ammonium acetate (20 mM, pH 6.8): acetonitrile of 90/10 to 10/90 over 20 min at a 1.0 mL/min flow rate.

Continuous wave (CW) electron paramagnetic resonance (EPR) spectra of the radicals (**Fig. S3**, red lines) were recorded using a Bruker EMX-plus X-band spectrometer at room temperature under anaerobic conditions. The instrumental settings were as follows: microwave power, 0.08 mW; time constant, 0.04 ms; modulation frequency, 100 kHz; modulation amplitude, 0.07 G. EPR measurements under anaerobic conditions were carried out by using a gas-permeable Teflon tube (i.d.=0.8 mm).

EPR spectral simulations (**Fig. S3**, black dotted lines) were carried out using the home-written EPR simulation program (ROKI\EPR) developed by Prof. Antal Rockenbauer.[S1-3] Simulation parameters are listed below. **CT02MA**: hyperfine splittings: 211 mG (1 ^{14}N), 89 mG (1 ^{1}H, unresolved) 48 mG (2 ^{1}H, unresolved), 1220 mG (3% ^{13}C), 2350 mG (6% ^{13}C), 3320 mG (3% ^{13}C), linewidth 60 mG. **OXMA**: hyperfine splittings: 207 mG (1 ^{14}N), 100 mG (1 ^{1}H, unresolved) 62 mG (2 ^{1}H, unresolved), 1100 mG (3% ^{13}C), 2390 mG (6% ^{13}C), 3470 mG (3% ^{13}C), linewidth 86 mG.

S2. Spin relaxation properties and Mims ENDOR spectra acquisition parameters

Table S1. Comparison of relaxation properties of different spin labeled proteins and Mims ENDOR acquisition parameters.

label	protein	tempera-ture, K	T_1, µs	stretched exponential β_1	T_M, µs	stretched exponential β_2	τ, µs	RF pulse length, µs	Shot repetition time, ms
Gd-DO3A	GB1 K31C	11	60	0.62	8.90	1.47	2	28	6
Gd-DO3A	GB1 Q32C	11	60	0.62	8.80	1.12	2.5	26	6
Gd-DO3A	Ub M1C	11	60	0.62	11.00	0.91	2	30	6
Gd-DO3A	Ub T66C	11	60	0.62	10.60	1.03	2	28	6
CT02MA	GB1 K31C	40	13200	1.01	2.50	1.28	2	40	20
OXMA	GB1 Q32C	40	18300	1.16	9.50	1.50	4	40	20
CT02MA	Ub M1C	40	10600	0.92	2.80	1.07	3	80	20
OXMA	Ub M1C	40	18500	1.11	6.70	1.30	3	40	20
CT02MA	Ub T66C	40	3980	0.77	2.40	1.34	2	40	20
MTSSL	GB1 K31C	40	2200	0.82	4.82	1.42	2	35	6
5-MSL	GB1 Q32C	40	1875	0.80	7.20	1.17	3	40	6
MTSSL	Ub M1C	40	2900	0.81	5.10	0.96	2	25	6
MTSSL	Ub T66C	25	10800	0.80	7.57	1.33	2	35	10
Cu-NTA	GB1 K28H Q32H	5	3500	0.74	5.00	1.10	2	35–40	3

S3. Comparison of spectra of OXMA and CT02MA

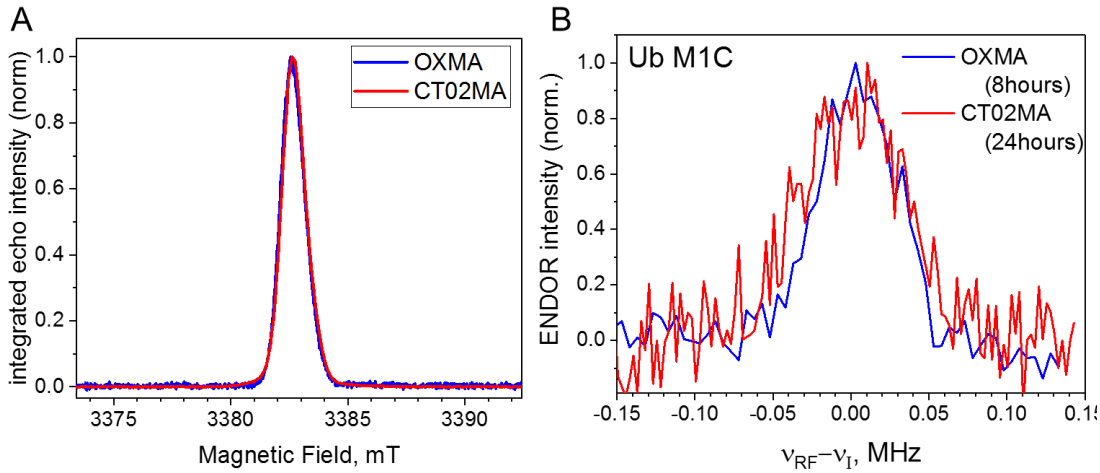

Fig. S4. ED- EPR (**A**) and ^{19}F ENDOR (**B**) spectra of Ub M1C labeled with OXMA (blue line) and CT02MA (red lines)

S4. Spectral simulations

Numerical simulations of ENDOR spectra were carried out using software described previously,[S4] which was modified to take into account the possibility of orientation selection with nitroxide and Cu–NTA labels, as previously described.[S3, S5, S6] In essence, the echo-detected EPR spectra of the samples were simulated initially using *g*- and hyperfine interaction tensors (assumed to be coaxial) as fitting parameters. The derived optimized parameters are listed in **Table S2**. Subsequently, the relative contributions of the different *g*-tensor orientations, selected at various field positions, were determined from EPR spectra simulations and used for ENDOR spectra simulations. It was assumed that the vector connecting the unpaired electron with the ^{19}F nucleus had a well-defined orientation in the *g*-tensor frame, parametrized by polar angles, θ_F and φ_F. The excitation bandwidth for the orientation selection depends on the MW $\pi/2$ pulse length used in the Mims sequence (leading to the experimentally used bandwidth of 50-60 MHz). However, it turned out that, for nitroxide labels, the ENDOR spectra were much more accurately simulated when a substantially larger excitation bandwidth was assumed (ca. 200 MHz). The most likely reason for this discrepancy is that orientational disorder of MTSSL labels within the protein causes an orientation distribution of the e-n dipolar vectors in the framework of nitroxide g-tensors. The exact degree of such orientation disorder is challenging to quantify, and using larger excitation bandwidth served as an efficient, albeit utterly phenomenological workaround.

Table S2. Principal values of the spin labels' g- and hyperfine interaction tensors, for which orientation selection was explicitly simulated.

	MTSSL GB1 K31C	MTSSL Ub T66C	Cu-NTA GB1 K28H Q32H
g_{xx}	2.0088	2.0085	2.0658
g_{yy}	2.0064	2.0063	2.0658
g_{zz}	2.0024	2.0026	2.2725
A_{xx}, MHz	14.4	14.8	–
A_{yy}, MHz	19.4	14.8	–
A_{zz}, MHz	100.3	97.9	120
θ_F, °	90	0	50
φ_F, °	0	0	–

S5. ^{19}F ENDOR spectra of nitroxide-labeled proteins acquired at different field positions

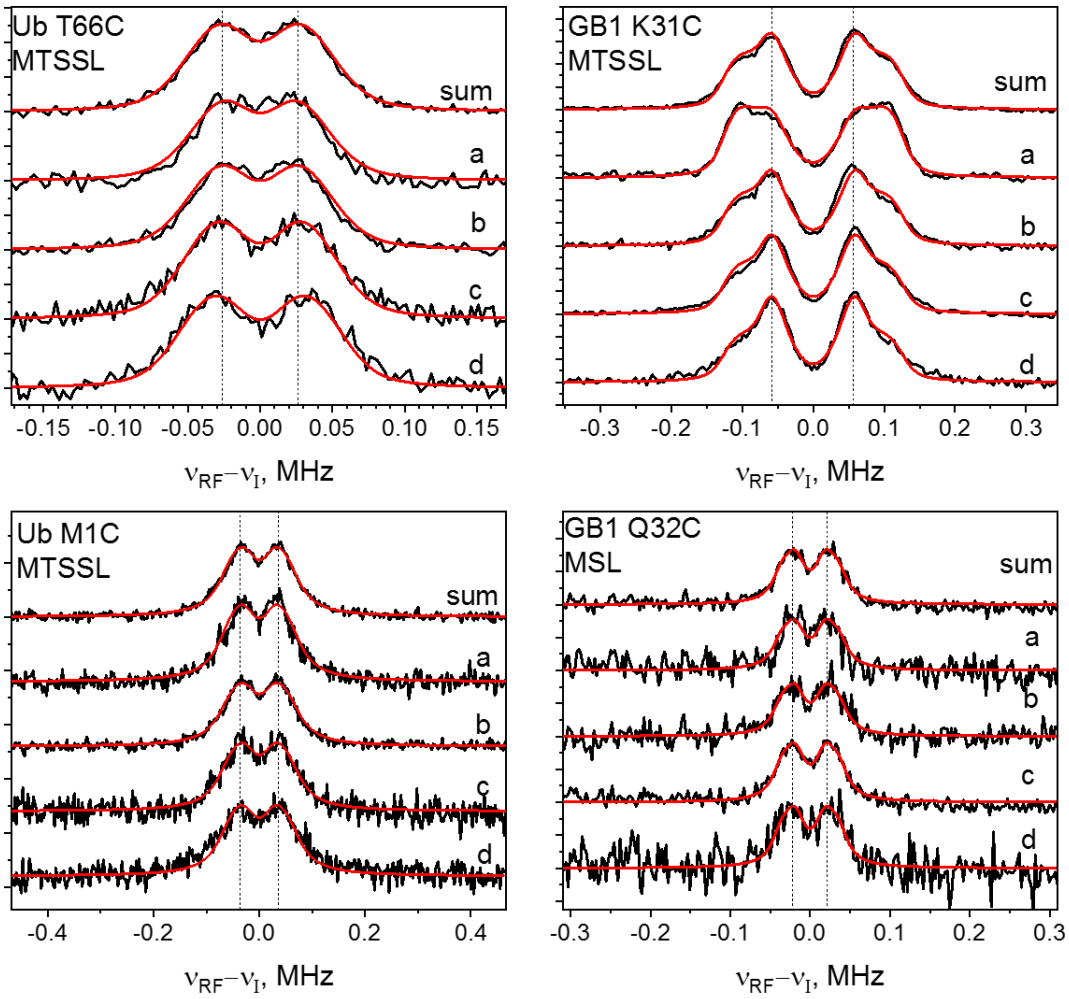

Fig. S5. Individual spectra of nitroxide labeled proteins (noted in each panel) recorded at various field positions (a, b, c, d; refer to Fig. 2A in the main text). Experimental spectra (black traces) and simulations (red traces) are superimposed. Vertical dashed lines, aligned with the maxima of the summed spectra, are shown to guide the eye.

Table S3. Simulation parameters of ^{19}F ENDOR spectra of various spin-labeled proteins.

label	protein	Single distance				Gaussian distance distribution	
		$a_\perp$,** kHz	r(e-n), Å	Lorentz lw, kHz	Gauss lw, kHz	r_0(e-n),*** Å	Δr,*** Å
Gd-DO3A	GB1 K31C	71.5	10.1	16.9	0	10.7	2.4
Gd-DO3A	GB1 Q32C	–	15.2*	–	–	–	–
Gd-DO3A	Ub M1C	63.9	10.5	17.8	0	11.3	2.8
Gd-DO3A	Ub T66C	37.1	12.6	24.1	0	16.2	6.4
CT02MA	GB1 K31C	40.0	12.3	12.8	0	12.6	2.0
OXMA	GB1 Q32C	–	–	–	–	–	–
OXMA	Ub M1C	–	–	–	–	–	–
CT02MA	Ub T66C	57.1	10.9	32.6	0	14.5	6.3
MTSSL	GB1 K31C	125.5	8.4	18.9	12.4	8.33	0.1
MSL	GB1 Q32C	40.5	12.2	14.7	0	13.3	3.5
MTSSL	Ub M1C	63.6	10.5	33	0	13.9	2.85
MTSSL	Ub T66C	54.0	11.1	11.6	28.2	14.0	6.4
Cu-NTA	GB1 K28H Q32H	46.1	11.7	1.8	23.4	–	–

*Gd-F distance as obtained from PRE[S7] and ENDOR measurement on the satellite transitions of Gd(III).[S4]

** $a_\perp$ is defined in eq. (1), main text.

*** Gaussian distribution center $\boldsymbol{r_0}$ and width $\boldsymbol{\Delta r}$, distribution probability density according to $dn/dr \propto \exp\left[-2\left(\frac{r-r_0}{\Delta r}\right)^2\right]$. Lorentzian line shape with the same width of 10 kHz was assumed in the simulations with the distance distribution for all proteins.

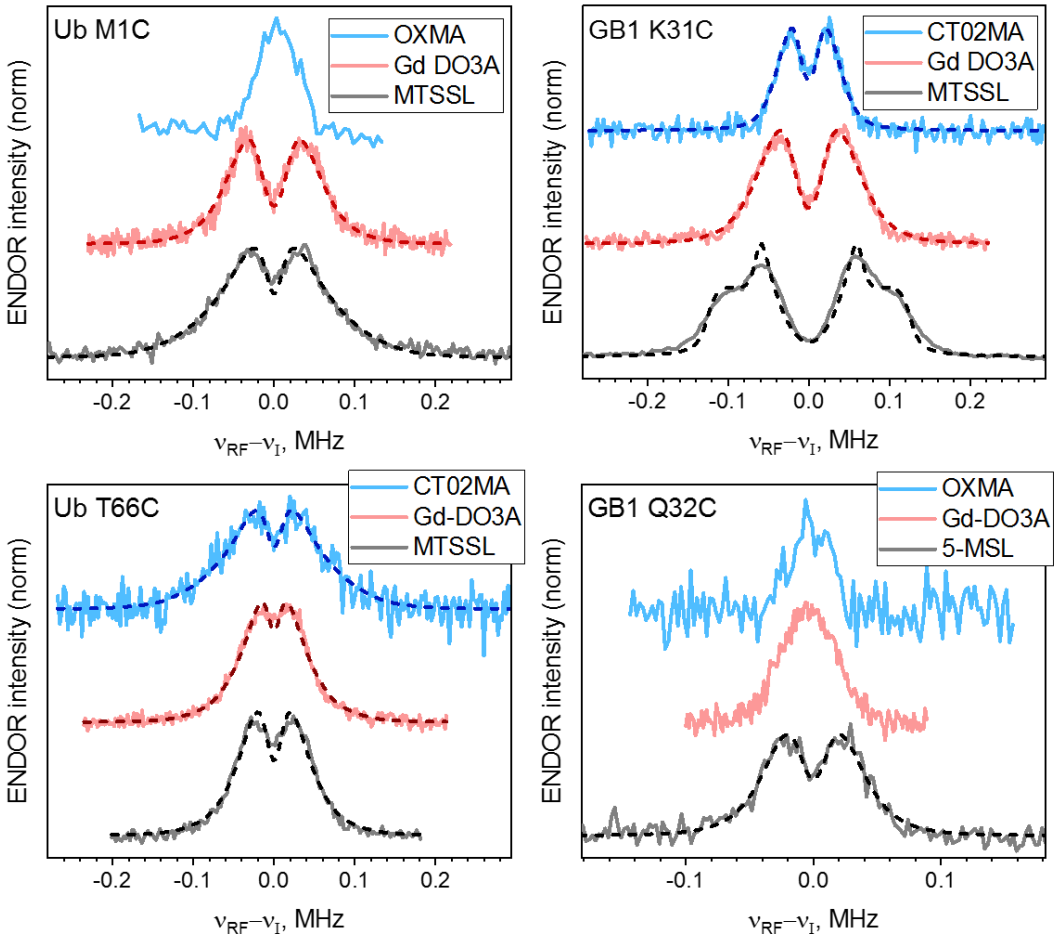

Fig. S6. Experimental spectra (solid lines) of the spin-labeled proteins (identical to those in **Fig. 3** of the main text) and their simulated counterparts (dashed lines). A Gaussian distribution of e-n distances and a fixed Lorentzian linewidth of 10 kHz was assumed for all spectra. The simulation parameters are listed in **Table S3**.

S5. Computational modeling of spin-labeled proteins conformations

Prediction of electron–fluorine distance distributions was performed using the ChiLife software.[S8] The rotamer library for the CT02MA label was computed using the CREST software[S9] at the GFN2-xTB[S10] level, using water as the solvent. The same rotamer library was used to simulate the OXMA spin label, which differs from CT02MA only by the flexible side groups, the inclusion of which in the rotamer library would be impractical.

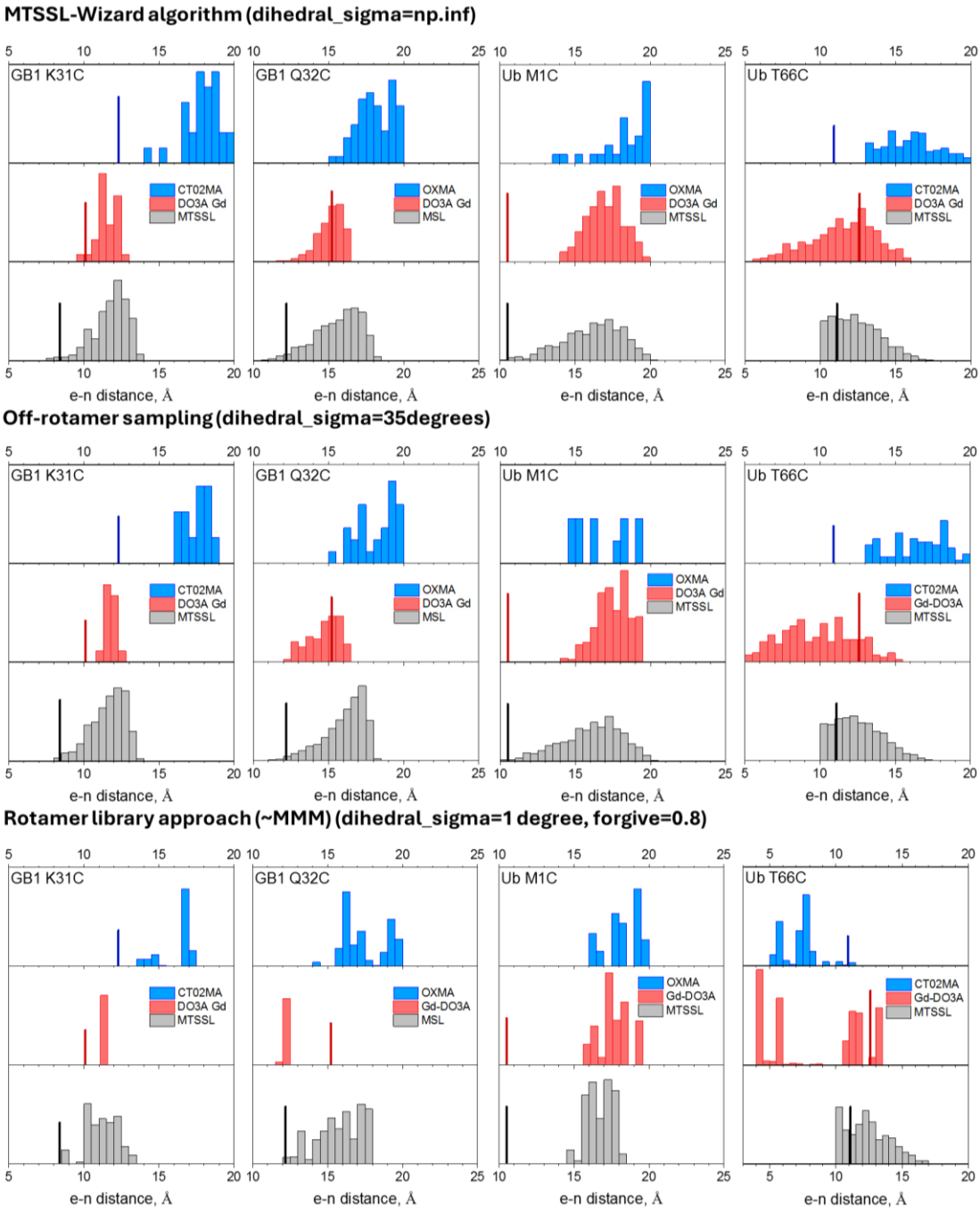

Fig. S7. Modeling of spin label rotamers using three computational approaches: free sampling of mobile dihedral angles top panels), off-rotamer sampling[S11] (middle panels) and the rotamer library approach (bottom panels); all results were obtained using the ChiLife software. Vertical lines correspond to the experimental distances obtained by simulation of ENDOR spectra using a single e-n distance approach, whereas the experimental Gd-F distance for GB1 Q32C Gd-DO3A is shown as obtained from PRE[S7] and ENDOR measurement on the satellite transitions of Gd(III).[S4]

S6. Comparison of the signal-to-noise ratio for various constructs

Table S4. Experimental signal-to-noise rations (SNR) of ^{19}F ENDOR spectra for the different samples, and other related parameters, namely: spectrometer used (cf **Section S3**), temperature, acquisition time, protein concentration, ENDOR efficiency F_{ENDOR}. Relative values of SNR predicted by equation (2) in main text are listed in the last column. Npts – number of points in the spectrum, sqrt(hrs) – square root of acquisition time.

label/field position	protein	spectro meter	temp eratu re, K	SNR of spectrum	Acquisi-tion time, hrs	SNR/ sqrt(hrs)	F_{ENDOR}, %	concent-ration, μM	Experimental SNR/sqrt(hrs)/ Npts/concent-ration, $\times 10^3$	rela-tive V_0*	rel. SNR_{ENDOR}, $\times 10^3$ (eq. (2), main text)	rel. SNR, $\times 10^3$ (eq. (2), main text)
Gd-DO3A	GB1 K31C	1	11	30.1	10.5	9.28	6.01	8	**4.64**	1.0	**9.66**	**9.66**
Gd-DO3A	GB1 Q32C	1	11	15.7	10	4.98	1.79	11	**2.98**	1.0	**2.37**	**2.37**
Gd-DO3A	Ub M1C	1	11	14.6	20.5	3.23	1.16	15	**0.72**	1.0	**1.66**	**1.66**
Gd-DO3A	Ub T66C	1	11	33.5	19	7.69	2.49	13	**1.97**	1.0	**3.77**	**3.77**
CT02MA	GB1 K31C	2	40	19.1	24.5	3.86	1.03	220	**0.07**	0.342	**0.37**	**0.13**
OXMA	GB1 Q32C	2	40	7.3	23.3	1.51	0.42	20	**0.62**	0.342	**0.44**	**0.15**
CT02MA	Ub M1C	2	40	7.2	21.3	1.57	0.57	110	**0.12**	0.342	**0.13**	**0.05**
OXMA	Ub M1C	1	40	16.8	8	5.94	1.17	110	**0.89**	0.342	**1.10**	**0.38**
CT02MA	Ub T66C	2	40	10.4	22	2.21	0.88	160	**0.06**	0.342	**0.26**	**0.09**
MTSSL a	GB1 K31C	1	40	25.6	7.1	9.61	7.42	95	**0.50**	0.0823	**13.60**	**1.12**
b				37.5	4.5	17.70	7.71	95	**0.47**	0.1487	**16.12**	**2.40**
c				56.5	5.8	23.45	8.01	95	**1.23**	0.1035	**18.64**	**1.93**
d				59.8	9	19.95	8.37	95	**1.05**	0.0558	**21.33**	**1.19**
5-MSL a	GB1 Q32C	1	40	7.7	14	2.06	1.21	120	**0.06**	0.0800	**2.11**	**0.17**
b				11.4	6	4.64	1.38	120	**0.14**	0.1487	**2.40**	**0.36**
c				11.6	16.3	2.87	1.13	120	**0.09**	0.106	**1.96**	**0.21**
d				7.4	5.3	3.21	1.66	120	**0.10**	0.0592	**2.89**	**0.17**
MTSSL a	Ub M1C	1	40	17.6	21.2	3.82	9.82	50	**0.19**	0.0753	**17.79**	**1.34**
b				25.8	9.7	8.29	7.40	50	**0.41**	0.1487	**13.40**	**1.99**
c				11.1	11.3	3.32	9.74	50	**0.17**	0.0858	**17.64**	**1.51**
d				12.1	29.3	2.24	8.75	50	**0.11**	0.0433	**15.84**	**0.69**
MTSSL a	Ub T66C	2	25	12.3	22	2.61	3.26	120	**0.14**	0.0986	**6.64**	**0.66**
b				14.2	16.3	3.53	2.98	120	**0.18**	0.1879	**7.43**	**1.40**
c				14.5	25.7	2.87	3.24	120	**0.15**	0.1134	**9.00**	**1.02**
d				14.2	53	1.96	3.26	120	**0.10**	0.0571	**8.74**	**0.50**
Cu-NTA g	GB1 K28H Q32H	2	5	18.6	11	5.61	3.54	420	**0.08**	0.085	**9.04**	**0.77**
a			5	8.0	53	1.10	4.34	420	**0.03**	0.0099	**11.05**	**0.11**

* The relative values of V_0 for each label were estimated experimentally by measuring the integrated spin echo intensity of 100 μM solutions of the corresponding free label in glycerol-d_8:D_2O (1:4). The values are given relative to Gd-DO3A at 11 K, taken as 1.0. The same value of V_0 was assumed for OXMA and CT02MA, and for 5-MSL and MTSSL. For nitroxides and Cu(II), V_0 was further normalized based on the relative EPR spectrum intensity at the corresponding magnetic field positions.

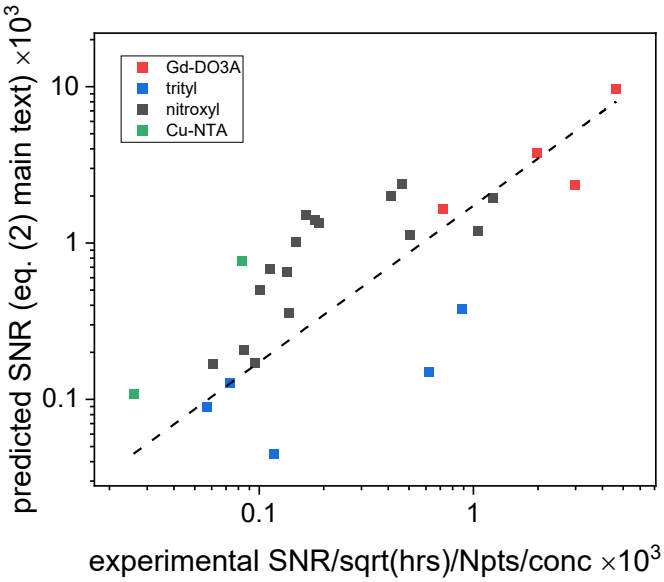

Fig. S8. Values of relative SNR predicted by eq. (2) in the main text, vs. experimentally obtained values of SNR per sqrt time, frequency point and concentration (corresponding values are listed in **Table S4** above). The dashed line corresponds to linear dependence with coefficient of determination R^2=0.84.

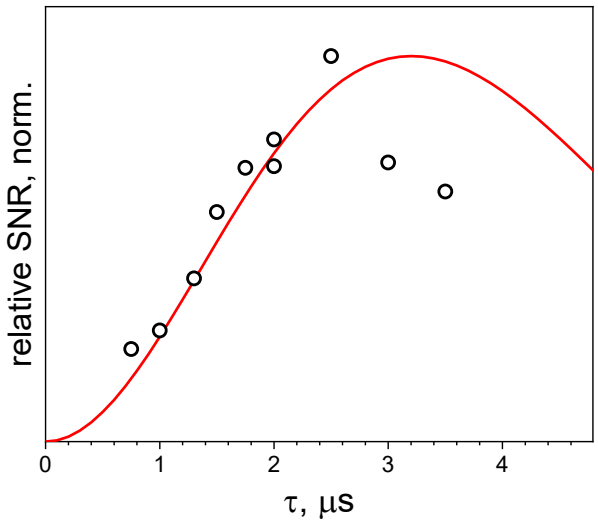

Fig. S9. Experimentally obtained values of SNR (black points) of ^{19}F ENDOR spectra of 240 μM GB1 K31C labeled with Gd-DO3A as a function of delay time τ in Mims ENDOR sequence and theoretical curve (red line) obtained from eq. (2) (main text) assuming that $F_{ENDOR} \propto \sin^2(\pi \cdot a\tau)$ calculated with the experimentally determined parameters T_M=6.3 μs, β_2=1.6, a=71.5 kHz. Both experimental and theoretical values are normalized.

References

S1. A. Rockenbauer and L. Korecz, *Applied Magnetic Resonance*, 1996, **10**, 29-43.

S2. A. Rockenbauer, T. Szabó-Plánka, Z. Árkosi and L. Korecz, *Journal of the American Chemical Society*, 2001, **123**, 7646-7654.

S3. H. Wiechers, A. Kehl, M. Hiller, B. Eltzner, S. F. Huckemann, A. Meyer, I. Tkach, M. Bennati and Y. Pokern, *J. Magn. Reson.*, 2023, **353**, 107491.

S4. A. Bogdanov, V. Frydman, M. Seal, L. Rapatskiy, A. Schnegg, W. Zhu, M. Iron, A. M. Gronenborn and D. Goldfarb, *Journal of the American Chemical Society*, 2024, **146**, 6157-6167.

S5. A. Meyer, A. Kehl, C. Cui, F. A. K. Reichardt, F. Hecker, L.-M. Funk, M. K. Ghosh, K.-T. Pan, H. Urlaub, K. Tittmann, J. Stubbe and M. Bennati, *J. Am. Chem. Soc.*, 2022, **144**, 11270-11282.

S6. A. Meyer, S. Dechert, S. Dey, C. Höbartner and M. Bennati, *Angew. Chem. Int. Ed.*, 2020, **59**, 373-379.

S7. M. Seal, W. Zhu, A. Dalaloyan, A. Feintuch, A. Bogdanov, V. Frydman, X.-C. Su, A. M. Gronenborn and D. Goldfarb, *Angew. Chem. Int. Ed.*, 2023, **62**, e202218780.

S8. M. H. Tessmer and S. Stoll, *PLOS Computational Biology*, 2023, **19**, e1010834.

S9. P. Pracht, F. Bohle and S. Grimme, *Phys. Chem. Chem. Phys.*, 2020, **22**, 7169-7192.

S10. C. Bannwarth, S. Ehlert and S. Grimme, *Journal of Chemical Theory and Computation*, 2019, **15**, 1652-1671.

S11. M. H. Tessmer, E. R. Canarie and S. Stoll, *Biophys. J.*, 2022, **121**, 3508-3519.